SCIENCE CHINA
Technological Sciences

•Article•

December 2020 Vol.63 No.12: 2664–2676
https://doi.org/10.1007/s11431-020-1613-0

Experimental definition and its significance on the minimum safe distance of blown sand between the proposed Qinghai-Tibet Expressway and the existing Qinghai-Tibet Railway

XIE ShengBo[1*], QU JianJun[1], HAN QingJie[1] & PANG YingJun[2]

[1] *Key Laboratory of Desert and Desertification, Dunhuang Gobi and Desert Research Station, Northwest Institute of Eco-Environment and Resources, Chinese Academy of Sciences, Lanzhou 730000, China;*
[2] *Institute of Desertification Studies, Chinese Academy of Forestry, Beijing 100091, China*

Received March 5, 2020; accepted April 24, 2020; published online July 23, 2020

The Qinghai-Tibet Expressway is a major strategic project planned by China that will be built along the Qinghai-Tibet Engineering Corridor. At present, important traffic line projects, such as the Qinghai-Tibet Railway, have been built within this narrow corridor, particularly at the blown sand sections. How to ensure that the wind speed and its flow field between the new expressway and existing railway subgrades are not affected by each other is a priority to prevent breaking the dynamic balance of the blown sand movement of the existing subgrade, thereby avoiding aggravating or inducing new blown sand hazards and ensure the safe operation of the existing Qinghai-Tibet Railway. Therefore, defining the minimum distance of the wind speed and its flow field, which are not affected by each other, between the subgrades become a scientific problem that should be solved immediately to implement the construction of the Qinghai-Tibet Expressway. For this purpose, the minimum safe distance between the subgrades of the Qinghai-Tibet Expressway and Qinghai-Tibet Railway was investigated from the perspective of blown sand by making subgrade models for conducting wind tunnel experiments and combining the observation data of the local field. Results indicated that the minimum safe distance between the two subgrades is 45–50 times the subgrade height when the Qinghai-Tibet Expressway is located at the downwind direction of the Qinghai-Tibet Railway, and 50 times the subgrade height when the former is located at the upwind direction of the latter. These results have guiding significance for the route selection, survey, and design of the Qinghai-Tibet Expressway at the blown sand sections and for the traffic line projects in other similar sandy regions.

Qinghai-Tibet Expressway, Qinghai-Tibet Railway, wind speed, wind flow field, safety distance

Citation: Xie S B, Qu J J, Han Q J, et al. Experimental definition and its significance on the minimum safe distance of blown sand between the proposed Qinghai-Tibet Expressway and the existing Qinghai-Tibet Railway. Sci China Tech Sci, 2020, 63: 2664–2676, https://doi.org/10.1007/s11431-020-1613-0

1 Introduction

Blown sand has constantly been an important factor perplexing the route selection, survey, design, construction, and safe operation of traffic line engineering in sandy regions [1–3]. Owing to the unique environment of the Qinghai-Tibet Plateau, which is characterized by high elevation, cold temperature, and blown sand [4–9], the blown sand hazards along the Qinghai-Tibet Railway are severe [10–12]. The Qinghai-Tibet Expressway is from Golmud to Lhasa, with a total length of approximately 1100 km, which is bound to be built along the existing Qinghai-Tibet Engineering Corridor (QTEC) because of limitations in the natural environment and construction conditions [13–15]. This narrow corridor is

*Corresponding author (email: xieshengbo@lzb.ac.cn)

only a few kilometers in its wide region and only a few hundred meters in its narrow region [16]. The existing projects, which are densely distributed within this corridor, mainly include the Qinghai-Tibet Railway, Qinghai-Tibet Highway, Qinghai-Tibet transmission and transformation lines, Qinghai-Tibet oil pipelines, and Lanzhou-Xining-Lhasa communication optical cables; among these projects, the Qinghai-Tibet Railway is the most remarkable and also the most important [17–19] (Figure 1). As the width of the expressway subgrade reaches 26 m and the pavement thickness is about 3 times that of the ordinary highways after it is built, the subgrade will significantly disrupt the original blown sand movement within the corridor and considerably change the near-surface blown sand flow field and conditions of transportation and accumulation [20]. If the distance is considerably close, then the expressway will also interact with the wind speed and flow field of other existing traffic lines within the corridor, particularly the subgrade of the Qinghai-Tibet Railway. Consequently, this situation will generate potential hazards. Accordingly, the distance of the proposed Qinghai-Tibet Expressway from the existing Qinghai-Tibet Railway should be determined before the construction of the expressway. At present, the relevant research in China and abroad mainly shown in these aspects, such as the law of blown sand accumulation over railway subgrade [21], the effect of railway bridge on wind-sand movement [22], the airflow field of opencut tunnel along railway [23],

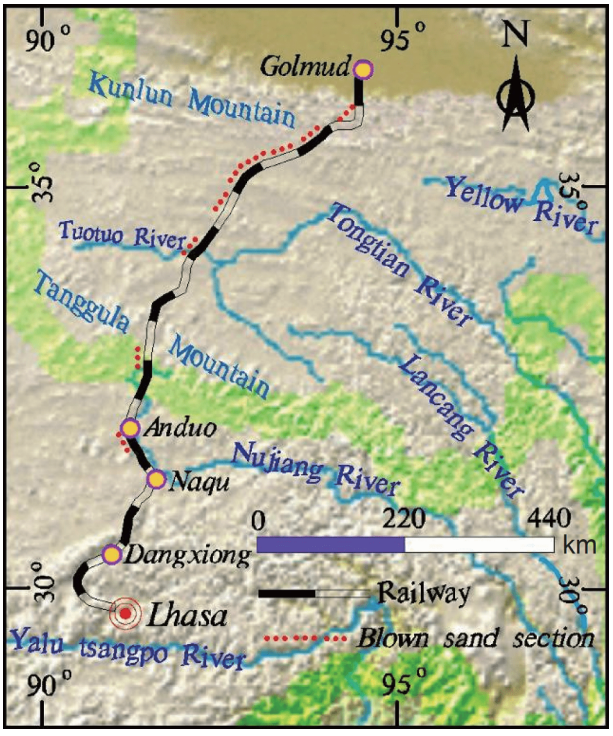

Figure 1 (Color online) Schematic map of the Qinghai-Tibet Railway (the base map comes from ref. [12]; Figure 1 is a modified drawing based on this base map).

wind erosion control of expressway embankment sideslopes [24], influence of dust emission on highway safety [3], blown sand-induced performance deficiencies of the railway and its prevention techniques [25], etc. These researches focus on the blown sand and its flow field of a single railway or highway line, many studies also have been conducted on the wind speed and flow field of a single-line subgrade of the Qinghai-Tibet Plateau [2,20,26]. However, only a few studies have been conducted on the wind speed and its flow field between the two line subgrades that interact with each other. Moreover, the definition of the safe distance of blown sand has yet to be reported. Therefore, by making subgrade models for conducting wind tunnel experiments, the authors attempted to define the minimum safe distance of blown sand between the Qinghai-Tibet Expressway and Qinghai-Tibet Railway.

2 Layout of wind tunnel experiment and methods

Experiments were conducted in a field mobile wind tunnel of the Key Laboratory of Desert and Desertification, Chinese Academy of Sciences (CAS). The wind tunnel has a test section that is 6 m in length and 0.63 m × 0.63 m cross-section. This tunnel is a direct current closed-blowing wind tunnel, and the wind speed could be continuously adjusted within the range of 0–20 m s^{-1}. The Qinghai-Tibet Railway is a class I single-track heavy railway based on the Design Specifications for Railway Subgrade (TB10001-2005, China). The top width of the subgrade is 3.5 m and the slope ratio is 1:1.75 (slope is 30°). According to the Highway Engineering Technique Standard (JTG B01-2014, China), the minimum top width of the subgrade of the proposed Qinghai-Tibet Expressway should be 26 m and the slope ratio should be 1:1.75 (slope is 30°). The subgrade models of the wind tunnel experiment were made in the proportion of 1:100. The size of the subgrade models are shown in Figure 2. The embankment of Qinghai-Tibet Railway is generally as high as 5–8 m due to need the cooling effect of crushed-rock interlayer [27,28], therefore, the height of the models is 8 cm and the length is 62 cm (Figure 2), the block ratio of the model is 12.5%.

The subgrade wind tunnel experiments were divided into two conditions: the expressway located at the downwind and upwind directions of the railway.

When the expressway was located at the downwind direction of the railway, the distance between the two subgrades was set as six groups: 10*H*, 20*H*, 30*H*, 40*H*, 50*H*, and 60*H*, where *H* represents the height of the subgrade model. An observation position was set every 5*H* distance between the two subgrades, and the wind speed at 10 different heights was measured using a pitot tube. The pitot tube was arranged

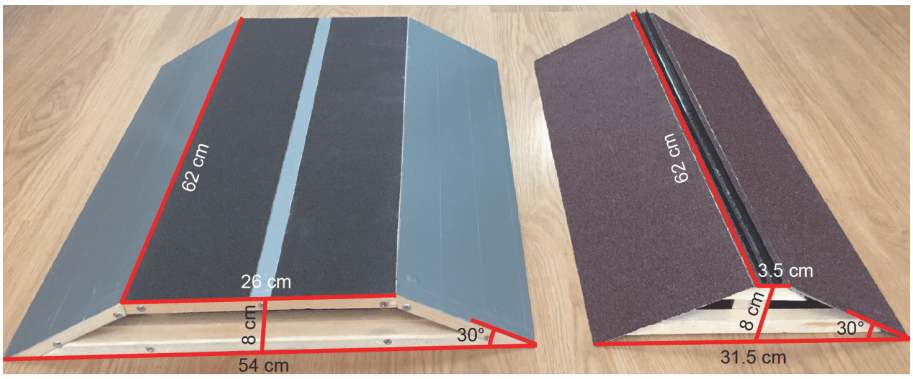

Figure 2 (Color online) Expressway and railway subgrade models.

at the center of the bottom plate of the wind tunnel, and the obtained heights were 0.6, 0.7, 1.3, 2.1, 8.3, 12.2, 16.4, 20.2, 24.2, and 28 cm after the experimental wind speed stabilized. Wind speed was measured once every 2 s for 30 consecutive times (i.e., 1 min), and the average value was taken as the result. Experimental wind speed is the wind speed at the center of the entrance of the experimental section of the wind tunnel. According to the observations of the local field, the sand-moving wind speed in the sandy region along the Qinghai-Tibet Railway is 5.7 m s^{-1} [29,30]. Therefore, the experimental wind speed was set as 6, 9, 12, 15, and 18 m s^{-1}. When the expressway was located at the upwind direction of the railway, the layout of the wind tunnel experiment was the same as that when the expressway was located at the downwind direction (Figures 3 and 4).

First, the initial wind speed profile without subgrade model in the wind tunnel (i.e., wind speed profile in the middle position of the wind tunnel experimental section under the five groups of the experimental wind speed) was measured before starting the subgrade wind tunnel experiment (Figure 5(a)). Wind speed at above 8.3 cm in height is stable, but that below 8.3 cm in height conforms to the logarithmic distribution law of wind speed with height on a uniform bed [31], which is expressed as follows:

$$u = \frac{u_*}{\kappa}\ln\frac{z}{z_0}, \tag{1}$$

where u is the wind speed at height z (m s^{-1}); κ is the Kaman constant (0.4); u_* is the frictional wind speed (m s^{-1}), and z_0 is the aerodynamic roughness (m).

$$u_* = \sqrt{\frac{\tau}{\rho}}, \tag{2}$$

where τ is the shear force or friction force between the ground and fluid (N m^{-2}) and ρ is the air density (kg m^{-3}). The fitted coefficients of wind speed profiles (below 8.3 cm) according to the eq. (1) were shown in Table 1.

Second, the initial sand transport rate without subgrade model in the wind tunnel (i.e., sand transport rate at the outlet of the wind tunnel experimental section under the five groups of the experimental wind speed) was measured (Figure 5(b)). The setting of the wind tunnel experiment to measure the sand transport rate is as follows: the sand bed was laid at the entrance of the experimental section of the wind tunnel, with a length of 3.6 m and a thickness of 5 cm; the middle is the expressway and the railway subgrade with a spacing of 10H, which is divided into two situations, i.e., the expressway located at the upwind and downwind directions of the railway; the sand collector was set at the outlet of the experi-

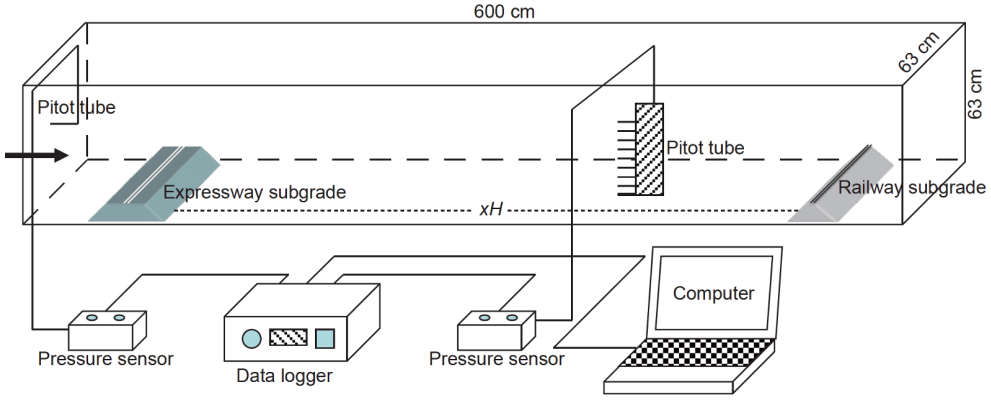

Figure 3 (Color online) Schematic the wind tunnel experiment layout.

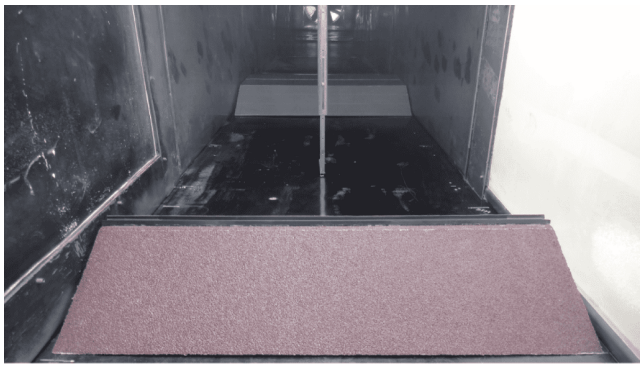

Figure 4 (Color online) Layout photograph of the wind tunnel experiment.

mental section of the wind tunnel (located at a distance of 10*H* away from the downwind direction of the downwind subgrade). The sand transport rate was measured 3 consecutive times, and the average value was taken as the result. The sand collector is a multi-channel flat mouth, an intake was set every 1 cm height with a total of 50 heights.

When the wind speeds in at least two observation positions (i.e., 5*H* distance) are equal and have been restored in the experimental results, the wind speed and its flow field between the two subgrades do not affect each other. Moreover, the corresponding subgrade spacing minus the distance of wind is speed equal and restoration is the minimum safe distance.

3 Results and analysis

3.1 Expressway located at the downwind direction of the railway

When the expressway was 60*H* away from the downwind direction of the railway, the variation of the wind speed at the downwind direction of the railway was obviously, the more close to the railway, the wind speed varies more obvious (Figure 6(a), (c), (e), (g), (i)), from the view of wind speed at each height, the wind speed decreased significantly when the height was less than and equal 12.2 cm, and the wind speed increased significantly when the height was greater than 12.2 cm. The wind speed of each height at the two observation positions of 35*H* and 45*H* had minimal difference, and the average values of the wind speed at the 10 heights were nearly the same (Figure 6(a), (c), (e), (g), (i), Table 2). Evidently, the wind speed between 35*H* and 45*H* was stable and had basically returned to the initial state. The flow field diagram indicates that the wind flow field between 35*H* and 45*H* was also basically restored (Figure 7). Therefore, the minimum safe distance should be 60*H* minus the 10*H*, which is 50*H*.

When the expressway was 50*H* away from the downwind

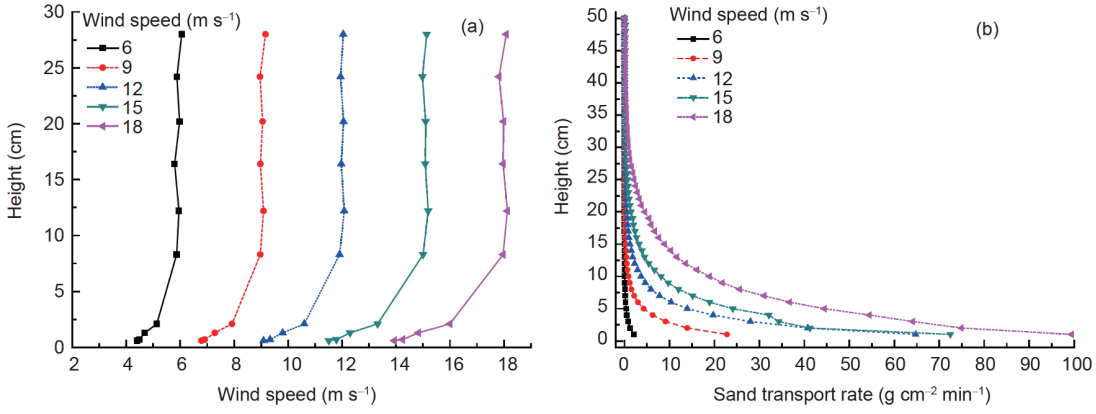

Figure 5 (Color online) Initial wind speed profile and sand transport rate. (a) Initial wind speed profile; (b) initial sand transport rate.

Table 1 The fitted coefficients of wind speed profiles (below 8.3 cm) according to the eq. (1)

Experimental wind speed (m s^{-1})	Frictional wind speed u_* (m s^{-1})	The aerodynamic roughness z_0 (mm)	R^2
6	0.23	0.0027	0.987
9	0.34	0.0020	0.991
12	0.43	0.0013	0.992
15	0.53	0.0011	0.990
18	0.62	0.0007	0.990

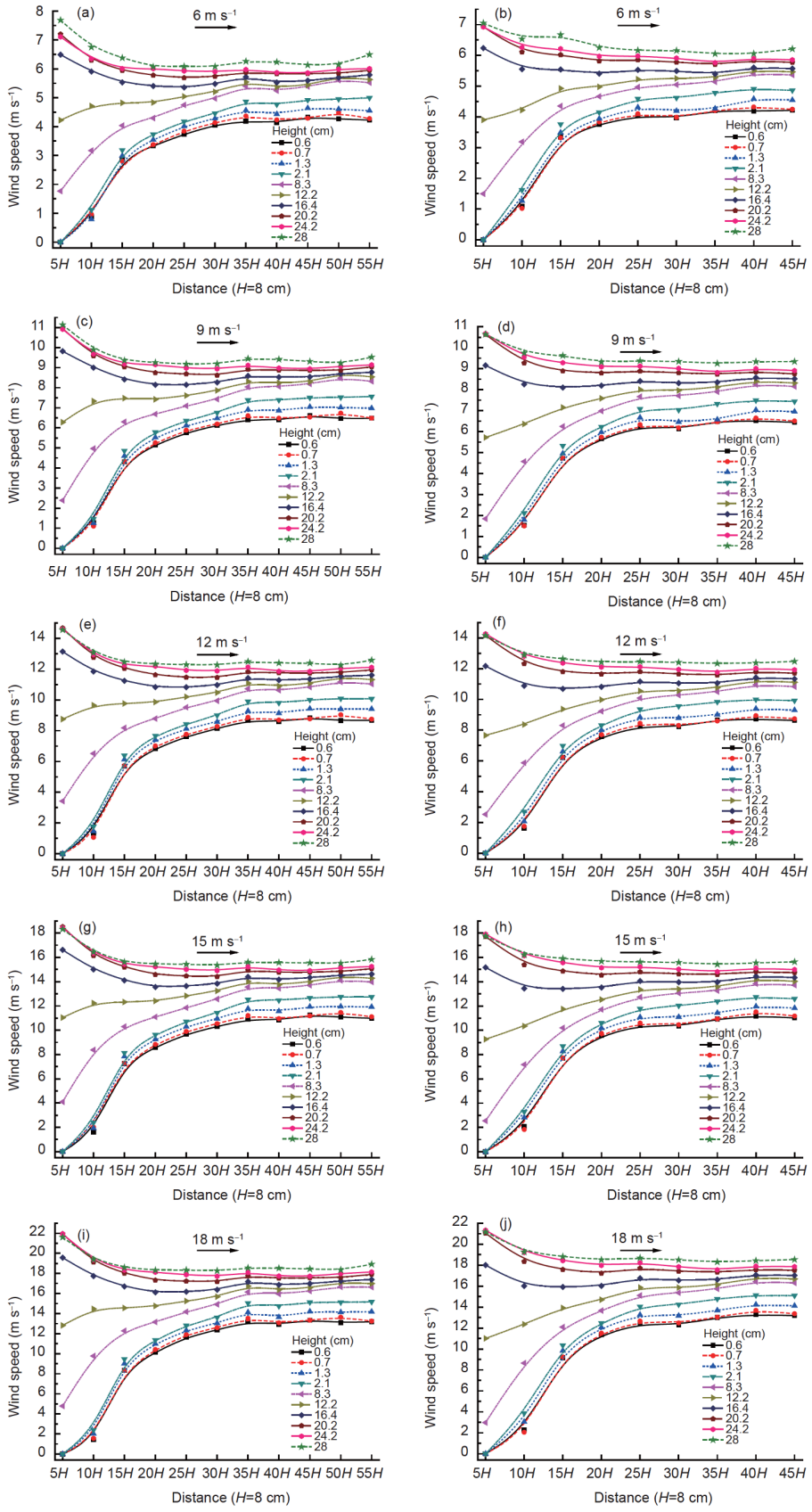

Figure 6 Wind speed of each observation point within the distance of 60*H* and 50*H* when the expressway is located at the downwind direction of the railway. (a) 60*H* distance, 6 m s^{-1}; (b) 50*H* distance, 6 m s^{-1}; (c) 60*H* distance, 9 m s^{-1}; (d) 50*H* distance, 9 m s^{-1}; (e) 60*H* distance, 12 m s^{-1}; (f) 50*H* distance, 12 m s^{-1}; (g) 60*H* distance, 15 m s^{-1}; (h) 50*H* distance, 15 m s^{-1}; (i) 60*H* distance, 18 m s^{-1}; (j) 50*H* distance, 18 m s^{-1}.

Table 2 The average values of the wind speed at the 10 heights of each observation point when the spacing are 60*H* and 50*H*

Position	Pacing	Experimental wind speed (m s^{-1})	The average values of the wind speed at the 10 heights of each observation point (m s^{-1})										
			5*H*	10*H*	15*H*	20*H*	25*H*	30*H*	35*H*	40*H*	45*H*	50*H*	55*H*
Expressway at downwind direction of railway	60*H*	6	3.4	3.7	4.5	4.6	4.9	5.0	**5.3**	5.2	**5.2**	5.3	5.3
		9	5.1	5.6	6.8	7.1	7.4	7.6	**8.0**	7.9	**8.0**	8.1	8.1
		12	6.9	7.2	9.0	9.5	9.8	10.1	**10.6**	10.5	**10.6**	10.7	10.8
		15	8.7	9.2	11.3	11.9	12.4	12.8	**13.4**	13.2	**13.4**	13.6	13.6
		18	10.3	10.7	13.4	14.1	14.8	15.2	**16.0**	15.7	**16.0**	16.1	16.2
	50*H*	6	3.3	3.7	4.8	4.9	5.1	5.0	5.1	**5.2**	**5.2**	–	–
		9	4.9	5.5	6.9	7.4	7.8	7.7	7.8	**8.0**	**7.9**	–	–
		12	6.5	7.1	9.1	9.8	10.3	10.3	10.4	**10.7**	**10.6**	–	–
		15	8.0	8.9	11.4	12.3	13.0	13.0	13.1	**13.5**	**13.4**	–	–
		18	9.6	10.5	13.5	14.5	15.5	15.4	15.6	**16.1**	**16.0**	–	–
Expressway at upwind direction of railway	60*H*	6	4.0	4.8	4.9	4.8	5.0	4.9	**5.1**	5.1	**5.1**	5.2	5.1
		9	6.1	7.2	7.4	7.2	7.4	7.5	**7.8**	7.6	**7.7**	7.9	7.6
		12	8.2	9.7	9.8	9.7	9.9	10.0	**10.5**	10.2	**10.3**	10.5	10.2
		15	10.3	12.3	12.4	12.1	12.5	12.6	**13.2**	12.9	**13.0**	13.2	12.9
		18	12.4	14.6	14.8	14.5	14.8	15.0	**15.6**	15.3	**15.5**	15.7	15.3
	50*H*	6	4.1	4.7	4.9	5.0	5.1	5.0	**5.1**	**5.1**	5.1	–	–
		9	6.2	7.0	7.4	7.5	7.8	7.6	**7.7**	**7.8**	7.7	–	–
		12	8.2	9.3	9.9	10.0	10.3	10.1	**10.3**	**10.4**	10.2	–	–
		15	10.4	11.6	12.4	12.5	13.0	12.7	**12.9**	**13.0**	12.8	–	–
		18	12.4	13.8	14.8	15.0	15.5	15.2	**15.4**	**15.5**	15.2	–	–

direction of the railway, the variation of the wind speed at the downwind direction of the railway was similar to that of the 60*H* distance (Figure 6(a), (c), (e), (g), (i)). The wind speed of each height at the two observation positions of 40*H* and 45*H* had minimal difference, and the average values of the wind speed at the 10 heights were nearly the same (Figure 6 (b), (d), (f), (h), (j), Table 2). Evidently, the wind speed between 40*H* and 45*H* was stable and had basically returned to the initial state. The flow field diagram indicates that the wind flow field between 40*H* and 45*H* was also basically restored (Figure 8). Therefore, the minimum safe distance should be 50*H* minus the 5*H*, which is 45*H*.

3.2 Expressway located at the upwind direction of the railway

When the expressway was 60*H* away from the upwind direction of the railway, the variation of the wind speed at the downwind direction of the expressway was obvious, particularly when the height was less than 8.3 cm, the more close to the expressway, the wind speed decreased more obvious (Figure 9(a), (c), (e), (g), (i)). The wind speed of each height at the two observation positions of 35*H* and 45*H* had minimal difference, and the average values of the wind speed at the 10 heights were nearly the same (Figure 9(a), (c), (e), (g), (i), Table 2). Evidently, the wind speed between 35*H* and 45*H* was stable and had basically returned to the initial state. The flow field diagram indicates that the wind flow field between 35*H* and 45*H* was also basically restored (Figure 10). Therefore, the minimum safe distance should be 60*H* minus the 10*H*, which is 50*H*.

When the expressway was 50*H* away from the upwind direction of the railway, the variation of the wind speed at the downwind direction of the expressway was obvious, particularly when the height was less than and equal 8.3 cm, the more close to the expressway, the wind speed decreased

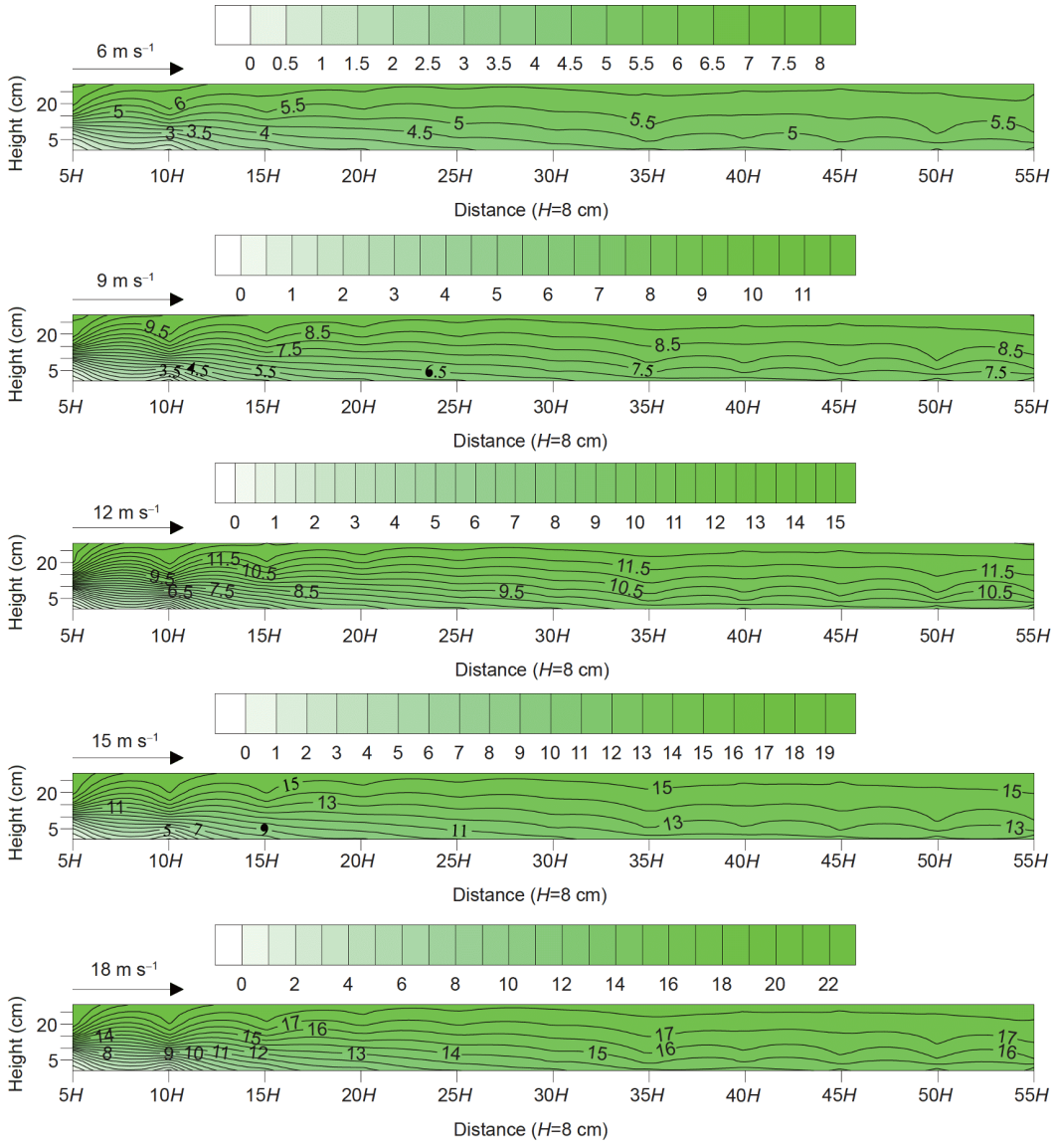

Figure 7 Wind flow field when the expressway is 60*H* away from the downwind direction of the railway.

more obvious (Figure 9(b), (d), (f), (h), (j)). The wind speed at each height of each observation position had a certain difference, particularly when the experimental wind speed was 6 m s^{-1}. The wind speed at a height of 28 cm (i.e., near the center of the experimental cross section of the wind tunnel) had a significant variation, and the wind speeds at other heights also had certain degrees of variations. The average values of the wind speed at the 10 heights of the two observation positions of 35*H* and 40*H* were nearly the same (Figure 9(b), (d), (f), (h), (j), Table 2). Clearly, the wind speed between 35*H* and 40*H* has yet to achieve full stability but considerably approximates the initial state in general. The flow field diagram indicates that the wind flow field between 35*H* and 40*H* was also near restoration (Figure 11).

The wind speed at the 10 heights and wind flow field between the two subgrades have remarkable difference compared with the initial state when the distances between the two subgrades were 10*H*, 20*H*, 30*H*, and 40*H*. This result holds regardless of whether the expressway was located at the downwind or upwind direction of the railway. The wind speed was unstable, and the wind flow field varied significantly. No case indicated that the wind speed at any two observation positions were approximately equal, the wind flow field did not return to its initial state, and the minimum safe distance was not within the range of 40*H*. Unfortunately, these aspects will not be discussed in this paper.

4 Discussion

Observations of the locale field indicate that the dominant wind direction along the Qinghai-Tibet Railway is westerly

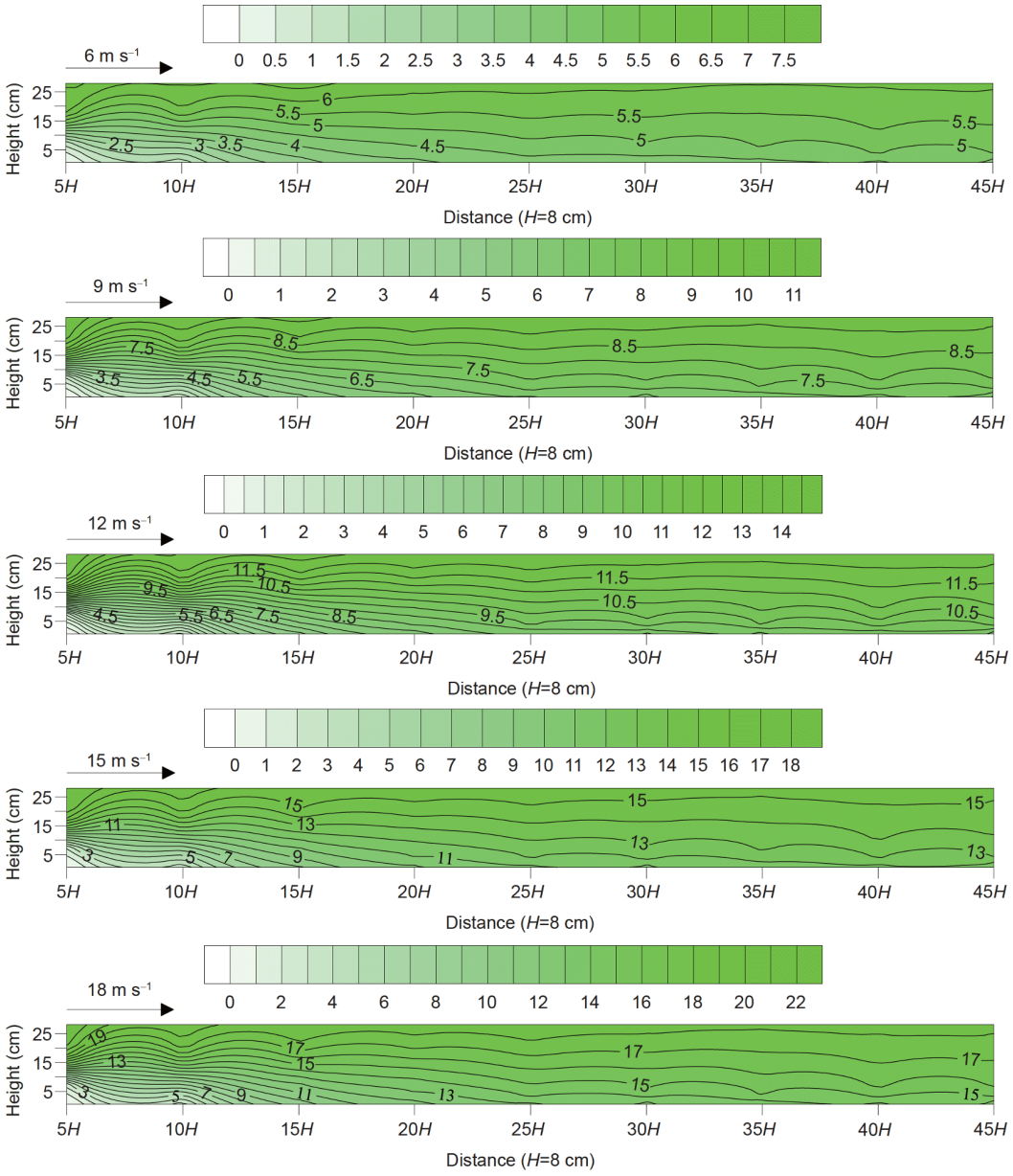

Figure 8 Wind flow field when the expressway is 50*H* away from the downwind direction of the railway.

[2], and the Qinghai-Tibet Railway (Golmud to Lhasa section) exhibits an approximately north-south trend (Figure 1). Therefore, the trend of the railway and proposed expressway is approximately perpendicular to the dominant wind direction [9]. The experiment setting of the wind tunnel is consistent with the reality from the view of the relationship between the dominant wind direction and line trend. The experimental results indicate that when the expressway is 60*H* away from the downwind direction of the railway, the wind speed of the 10*H* distance from 35*H* to 45*H* regained stability. However, the section where the wind speed regained stability was larger than the length of the 10*H*, and the corresponding safety distance was less than 50*H*. While when the expressway is 50*H* away from the downwind direction of the railway, the wind speed of the 5*H* distance from 40*H* to 45*H* regained stability. However, the section where the wind speed regained stability was less than the length of the 5*H*, and the corresponding safety distance was greater than 45*H*. The section less than 5*H* was not observed because the interval distance between the observation positions is 5*H*, which can also be confirmed by the wind speed and its flow field diagram of each observation position (Figures 6–8). By considering these two results comprehensively, the minimum safe distance between the two subgrades should be between 45*H* and 50*H* when the expressway was located at the downwind direction of the railway. Similarly, when the expressway was located at the upwind direction of the railway, the minimum safe distance

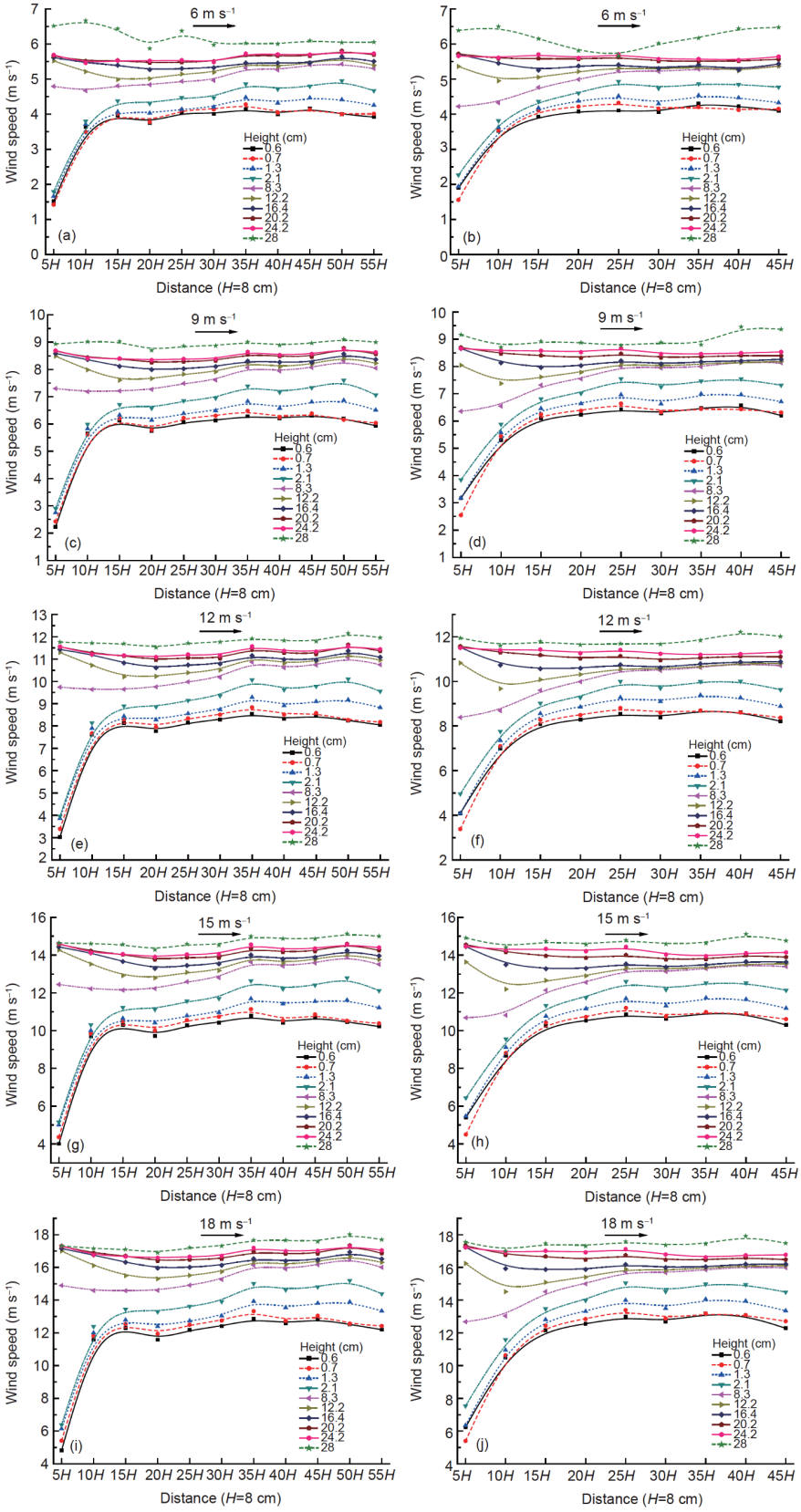

Figure 9 Wind speed of each observation point within the distance of 60*H* and 50*H* when the expressway is located at the upwind direction of the railway. (a) 60*H* distance, 6 m s^{-1}; (b) 50*H* distance, 6 m s^{-1}; (c) 60*H* distance, 9 m s^{-1}; (d) 50*H* distance, 9 m s^{-1}; (e) 60*H* distance, 12 m s^{-1}; (f) 50*H* distance, 12 m s^{-1}; (g) 60*H* distance, 15 m s^{-1}; (h) 50*H* distance, 15 m s^{-1}; (i) 60*H* distance, 18 m s^{-1}; (j) 50*H* distance, 18 m s^{-1}.

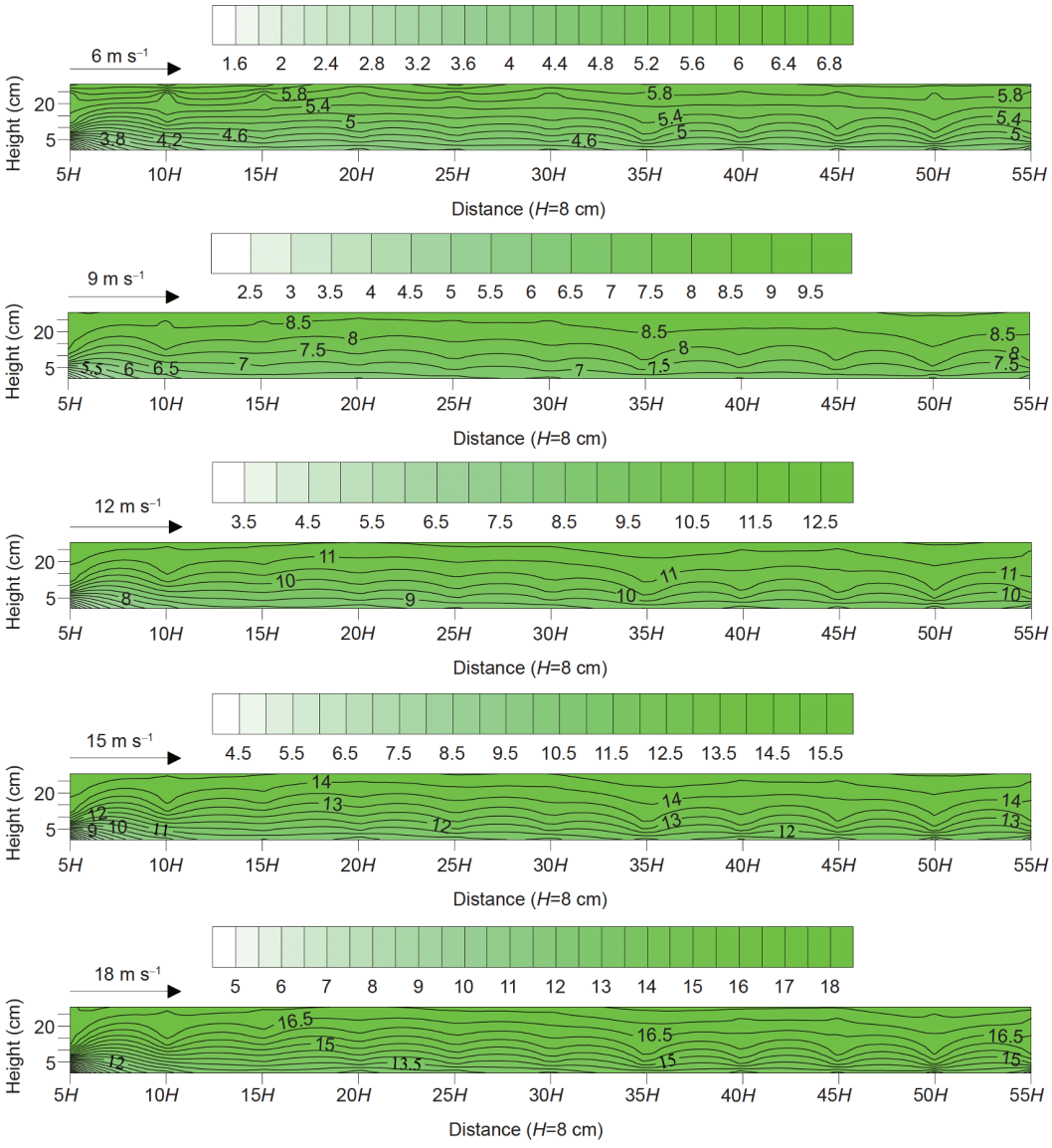

Figure 10 Wind flow field when the expressway is 60*H* away from the upwind direction of the railway.

between the two subgrades was 50*H*. In addition, when the expressway was 60*H* and 50*H* away from the upwind direction of the railway, the surface roughness of the railway subgrade located at the downwind direction is considerably large. This result has an evident weakening effect on the wind speed near the ground. Hence, the outcome is a significant decrease in wind speed near the ground (particularly at height below 2.1 cm) at 55*H* and 45*H* (i.e., −5*H* upwind direction of the railway) away from the downwind direction of the expressway. Meanwhile, the blocking and weakening effects on wind was strong and part of the wind energy was consumed because of the wide expressway subgrade located at the upwind direction. Consequently, the average value of the wind speed at the 10 heights at the observation positions of 35*H*, 40*H*, and 45*H* was lower than the corresponding average value when the expressway was located at the downwind direction (Table 2). Moreover, the wind speed fluctuation at each height was evident. Therefore, the needed distance for wind speed and its flow field to return to the stable initial state is longer when the expressway is located at the upwind direction of the railway compared with the downwind direction. Accordingly, the minimum safe distance when the expressway located at the upwind direction of the railway is slightly longer than that of the minimum safe distance when the expressway is located at the downwind direction of the railway.

According to the measurement results of the sand transport rate at the outlet of the experimental section of the wind tunnel, the sand transport rate under the 5 groups of the experimental wind speed when the expressway is 10*H* away from the downwind direction of the railway were 2.89, 35.89, 139.96, 237.30, 363.48 g cm^{-2} min^{-1}, respectively, and the sand

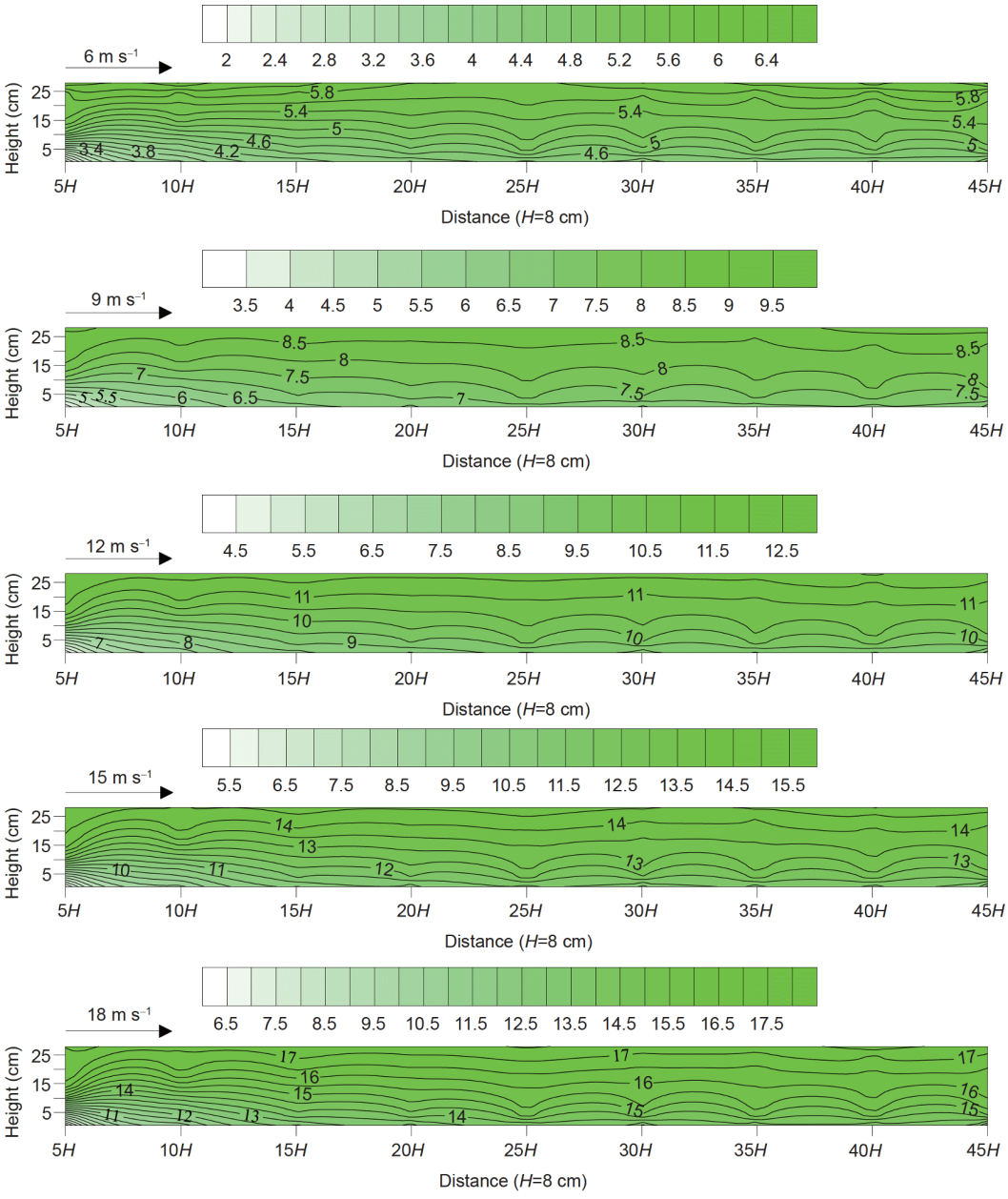

Figure 11 Wind flow field when the expressway is 50*H* away from the upwind direction of the railway.

transport rate under the 5 groups of the experimental wind speed when the expressway is 10*H* away from the upwind direction of the railway were 1.91, 41.34, 113.03, 201.36, 303.86 g cm^{-2} min^{-1}, respectively. The sand transport rate when the expressway is 10*H* away from the downwind direction of the railway is generally higher than that of the sand transport rate when the expressway is 10*H* away from the upwind direction of the railway (Figure 12). This finding shows that the passing rate of the blown sand flow when the expressway located at the downwind direction is high, and the disturbance intensity to the blown sand movement is lower than that of the upwind direction.

5 Conclusions

The following conclusions can be drawn under the experimental conditions.

The minimum safe distance between the two subgrades is 45–50 times of the subgrade height when the Qinghai-Tibet Expressway is located at the downwind direction of the Qinghai-Tibet Railway, and 50 times of the subgrade height when the Qinghai-Tibet Expressway is located at the upwind direction of the Qinghai-Tibet Railway.

Several traffic lines can only pass through the same corridor in some regions, such as QTEC, South Tibet Alpine

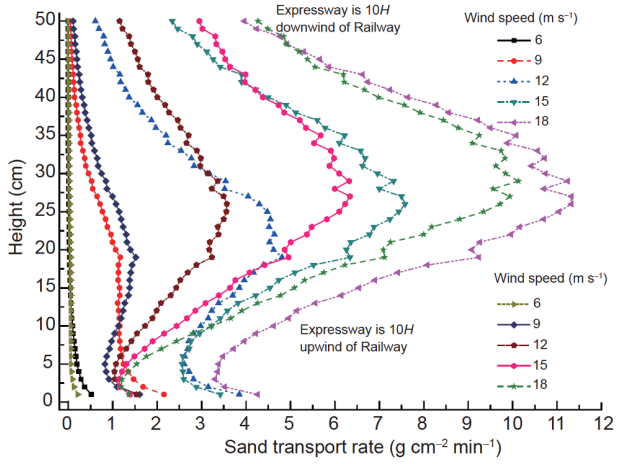

Figure 12 Sand transport rate when the expressway is 10*H* away from the downwind and upwind direction of the railway.

Valley, and Hexi Corridor, with the rapid development of the construction of the traffic line project in the sandy regions owing to the limitations of the natural environment and construction conditions [32]. Thus, urgent scientific problems should be solved to avoid aggravating or inducing new blown sand hazards. Among these problems are related to surveying and designing a new traffic line project within the same corridor or valley where existing lines are densely distributed in the blown sand regions, and ensuring that wind speed and its flow field between the line subgrades are not affected by each other. The minimum safe distance of blown sand between the proposed expressway and existing railway within QTEC was defined clearly by the aforementioned experimental results and analysis. This research has important significance for the route selection, survey, and design of the Qinghai-Tibet Expressway at the blown sand sections and of traffic line projects in other similar sandy regions.

This work was supported by the National Natural Science Foundation of China (Grant No. 41877530), the Youth Innovation Promotion Association CAS (Grant No. 2018459). The authors would like to thank the three anonymous reviewers' useful comments and the editor's valuable suggestions for improving this manuscript.

1 Zhang K C, Qu J J, Han Q J, et al. Wind tunnel simulation of wind-blown sand along China's Qinghai-Tibet Railway. Land Degrad Develop, 2014, 25: 244–250
2 Xie S B, Qu J J, Lai Y M, et al. Formation mechanism and suitable controlling pattern of sand hazards at Honglianghe River section of Qinghai-Tibet Railway. Nat Hazards, 2015, 76: 855–871
3 Li J, Kandakji T, Lee J A, et al. Blowing dust and highway safety in the southwestern United States: Characteristics of dust emission "hotspots" and management implications. Sci Total Environ, 2018, 621: 1023–1032
4 Tapponnier P, Xu Z Q, Roger F, et al. Oblique stepwise rise and growth of the Tibet Plateau. Science, 2001, 294: 1671–1677
5 Liu Z M, Zhao W Z. Shifting-sand control in central Tibet. AMBIO-A J Human Environ, 2001, 30: 376–380
6 Yan P, Dong Z B, Dong G R, et al. Preliminary results of using ^{137}Cs to study wind erosion in the Qinghai-Tibet Plateau. J Arid Environ, 2001, 47: 443–452
7 Wang G X, Li Y S, Wu Q B, et al. Impacts of permafrost changes on alpine ecosystem in Qinghai-Tibet Plateau. Sci China Ser D-Earth Sci, 2006, 49: 1156–1169
8 Yang M X, Yao T D, Gou X H, et al. Diurnal freeze/thaw cycles of the ground surface on the Tibetan Plateau. Chin Sci Bull, 2007, 52: 136–139
9 Xie S B, Qu J J, Pang Y J. Dynamic wind differences in the formation of sand hazards at high- and low-altitude railway sections. J Wind Eng Ind Aerodyn, 2017, 169: 39–46
10 Liu L, Liu S H, Xu Z Y. Efficiency of wind erosion control measures at the Dk1562 section of the Qinghai-Tibet Railway. In: The International Specialty Conference on Science and Technology for Desertification Control. Beijing, 2006. 223–229
11 Zhang K C, Qu J J, Liao K T, et al. Damage by wind-blown sand and its control along Qinghai-Tibet Railway in China. Aeolian Res, 2010, 1: 143–146
12 Xie S B, Qu J J, Zu R P, et al. Effect of sandy sediments produced by the mechanical control of sand deposition on the thermal regime of underlying permafrost along the Qinghai-Tibet Railway. Land Degrad Develop, 2013, 24: 453–462
13 Zou X Y, Li S, Zhang C L, et al. Desertification and control plan in the Tibet Autonomous Region of China. J Arid Environ, 2002, 51: 183–198
14 Zhang C L, Zou X Y, Yang P, et al. Wind tunnel test and ^{137}Cs tracing study on wind erosion of several soils in Tibet. Soil Tillage Res, 2007, 94: 269–282
15 Liu D, Wang T, Yang T, et al. Deciphering impacts of climate extremes on Tibetan grasslands in the last fifteen years. Sci Bull, 2019, 64: 446–454
16 Zhang M Y, Pei W S, Zhang X Y, et al. Lateral thermal disturbance of embankments in the permafrost regions of the Qinghai-Tibet Engineering Corridor. Nat Hazards, 2015, 78: 2121–2142
17 Shen W S, Zhang H, Zou C X, et al. Approaches to prediction of impact of Qinghai-Tibet Railway construction on alpine ecosystems alongside and its recovery. Chin Sci Bull, 2004, 49: 834–841
18 Wang G X, Yao J Z, Guo Z G, et al. Changes in permafrost ecosystem under the influences of human engineering activities and its enlightenment to railway construction. Chin Sci Bull, 2004, 49: 1741–1750
19 Xie S B, Qu J J, Mu Y H, et al. Variation and significance of surface heat after the mechanical sand control of Qinghai-Tibet Railway was covered with sandy sediments. Results Phys, 2017, 7: 1712–1721
20 Zhang K C, Qu J J, Niu Q H, et al. Characteristics of wind-blown sand and dynamic environment in the section of Wudaoliang-Tuotuo River along the Qinghai-Tibet Railway. Environ Earth Sci, 2011, 64: 2039–2046
21 Huang N, Gong K, Xu B, et al. Investigations into the law of sand particle accumulation over railway subgrade with wind-break wall. Eur Phys J E, 2019, 42: 145
22 He W, Huang N, Xu B, et al. Numerical simulation of wind-sand movement in the reversed flow region of a sand dune with a bridge built downstream. Eur Phys J E, 2018, 41: 53
23 Yan M, Wang H B, Zuo H J, et al. Wind tunnel simulation of an opencut tunnel airflow field along the Linhe-Ceke Railway, China. Aeolian Res, 2019, 39: 66–76
24 Hu L, Shan Y T, Chen R H, et al. A study of erosion control on expressway embankment sideslopes with three-dimensional net seeding on the Qinghai-Tibet Plateau. CATENA, 2016, 147: 463–468
25 Bruno L, Horvat M, Raffaele L. Windblown sand along railway infrastructures: A review of challenges and mitigation measures. J Wind Eng Ind Aerodyn, 2018, 177: 340–365
26 Xiao J H, Yao Z Y, Qu J J. Influence of Golmud-Lhasa section of Qinghai-Tibet Railway on blown sand transport. Chin Geogr Sci, 2015, 25: 39–50
27 Lai Y M, Zhang M Y, Liu Z Q, et al. Numerical analysis for cooling

effect of open boundary ripped-rock embankment on Qinghai-Tibetan railway. Sci China Ser D-Earth Sci, 2006, 49: 764–772
28 Cheng G D, Wu Q B, Ma W. Innovative designs of permafrost roadbed for the Qinghai-Tibet Railway. Sci China Ser E-Tech Sci, 2009, 52: 530–538
29 Han Q J, Qu J J, Dong Z B, et al. Air density effects on aeolian sand movement: implications for sediment transport and sand control in regions with extreme altitudes or temperatures. Sedimentology, 2015, 62: 1024–1038
30 Han Q J, Qu J J, Dong Z B, et al. The effect of air density on sand transport structures and the adobe abrasion profile: A field wind-tunnel experiment over a wide range of altitude. Bound-Layer Meteorol, 2014, 150: 299–317
31 Bagnold R A. The Physics of Blown Sand and Desert Dunes. Mineola, New York: Dover Publications, Inc., 2005. 47–49
32 Chen R D, Liu X N, Cao S Y, et al. Numerical simulation of deposit in confluence zone of debris flow and mainstream. Sci China Tech Sci, 2011, 54: 2618–2628